Received: 22 June 2021 | Accepted: 18 November 2021

DOI: 10.1111/jvim.16331

STANDARD ARTICLE

Journal of Veterinary Internal Medicine Open Access

ACVIM American College of Veterinary Internal Medicine

Echocardiographic reference intervals for right ventricular indices, including 3-dimensional volume and 2-dimensional strain measurements in healthy dogs

Elisabeth K. Feldhütter[1] | Oriol Domenech[2] | Tommaso Vezzosi[2,3] | Rosalba Tognetti[3] | Nadja Sauter[4] | Alexander Bauer[4] | Jenny Eberhard[1] | Jana Friederich[1] | Gerhard Wess[1]

[1]Clinic of Small Animal Medicine, LMU University, Munich, Germany

[2]Anicura Istituto Veterinario Novara, Novara, Italy

[3]Department of Veterinary Sciences, University of Pisa, Pisa, Italy

[4]Statistical Consulting Unit StaBLab, LMU University, Munich, Germany

Correspondence
Gerhard Wess, Clinic of Small Animal Medicine, LMU University, Veterinaerstr. 13, 80539 Munich, Germany.
Email: gwess@lmu.de

Abstract

Background: There is currently a lack of reference intervals (RIs) for the novel measures like 3-dimensional (3D) echocardiography or speckle-tracking strain for assessment of right ventricular (RV) structure and function.

Objectives: To generate RIs and to determine the influence of age, heart rate, and body weight (BW) on various RV function indices using a dedicated RV software for 3D RV end-diastolic volume (EDV), end-systolic volume (ESV), ejection fraction (EF), global and free wall RV longitudinal strain (RVLS), end-diastolic area (RVEDA), end-systolic area (RVESA), fractional area change (FAC), tricuspid annular plane systolic excursion (TAPSE), and tissue Doppler imaging (TVI)-derived systolic myocardial velocity of the lateral tricuspid annulus (S′).

Animals: Healthy adult client-owned dogs (n = 211) of various breeds and ages.

Methods: Prospective study. Reference intervals were estimated as statistical prediction intervals using allometric scaling for BW-dependent variables. Right-sided (upper limit) or left-sided (lower limit) 95% RIs were calculated for every variable. Inter- and intraobserver variability was determined.

Results: Most variables showed clinically acceptable repeatability with coefficient of variation less than 10. Upper or respectively lower RI after allometric scaling to normalize for different BWs were: EDVn ≤ 2.5 $mL/kg^{0.942}$, ESVn ≤ 1.2 $mL/kg^{0.962}$, TAPSEn ≥ 4.5 $mm^{0.285}$, RVEDAn ≤ 1.4 $cm^2/kg^{0.665}$, RVESAn ≤ 0.8 $cm^2/kg^{0.695}$, and TVI S′n ≥ 5.6 $cm/s/kg^{0.186}$. The calculated limits for indices without allometric normalization were: EF > 42.1%, FAC > 30.0%, free wall RVLS < −20.8%, and global RVLS < −18.3%.

Abbreviations: 2D, 2-dimensional; 3D, 3-dimensional; BSA, body surface area; BW, body weight; CLSI, Clinical and Laboratory Standards Institute; CV, coefficient of variation; EDV, RV end-diastolic volume; EF, ejection fraction; ESV, RV end-systolic volume; FAC, fractional area change; HR, heart rate; LV, left ventricle; MRI, magnetic resonance imaging; PH, pulmonary hypertension; PIs, prediction intervals; RI, reference interval; RV, right ventricle; RVEDA, RV end-diastolic area; RVESA, RV end-systolic area; RVLS, right ventricular longitudinal strain STE, speckle-tracking echocardiography; TAPSE, tricuspid annular plane systolic excursion; TTE, transthoracic echocardiography; TVI S′, tissue Doppler imaging-derived systolic myocardial velocity of the lateral tricuspid annulus.

Conclusions: Echocardiographic RIs for RV structure and function are provided.

KEYWORDS
canine, heart dimensions, prediction intervals, repeatability, volumetric measurements

1 | INTRODUCTION

Quantitative assessment of cardiac function focuses on the left ventricle (LV) with the right ventricle (RV) being less well studied. The RV plays an important role in many diseases affecting left heart,[1,2] right heart,[3,4] and causing pulmonary hypertension (PH).[5-7]

Accurate assessment of the RV is challenging because of its complex geometry. The strong apical trabeculation, crescent shape, and a missing fibrous continuity between its inlet and outlet areas make it difficult to determine RV structures using echocardiography.[8-10]

Although magnetic resonance imaging (MRI) represents the noninvasive reference standard for imaging cardiac function and mass in human medicine as well as in dogs,[11-13] echocardiography remains the commonly used noninvasive method for evaluation of cardiac and RV function. Because of its noninvasive nature, its wide accessibility, and no need for general anesthesia, echocardiography is well established for the assessment of RV function.

Some of the commonly used variables for RV function are M-Mode-derived tricuspid annular plane systolic excursion (TAPSE),[14] fractional area change (FAC),[15] and tissue Doppler imaging (TVI)-derived systolic myocardial velocity of the lateral tricuspid annulus (S′).[16] A more recently introduced variable is strain measurement derived by speckle-tracking echocardiography (STE). Using this method, regional and global myocardial deformation can be evaluated, allowing conclusions about RV systolic function.[17]

Another promising variable in humans is RV volume derived by 3-dimensional (3D) transthoracic echocardiography (TTE). There is good agreement between RV volumetric quantification using cardiac MRI and 3D TTE, the latter resulting in smaller volumes.[10,18-20] Similar results have been achieved in animals where, despite of its slight underestimation, 3D TTE is a good alternative for quantification of RV volumes because of its excellent agreement with cardiac MRI.[13,20]

Strain measurements and 3D volume offer relevant advantages over conventional methods such as TAPSE or FAC. Strain provides an angle-independent variable[21] evaluating the entire RV without only including 1 regional segment compared to TAPSE or TVI S′. 3D TTE provides accurate volume quantification avoiding geometrical assumption.[13,20]

Studies are needed providing reference intervals (RIs) for 3D TTE derived RV volumes in dogs. There are several studies that estimated RI in dogs for conventional variables such as TVI S′, TAPSE, and FAC.[3,14,22,23] In healthy dogs, 2-dimensional (2D) RV transverse strain and strain rate was assessed[24] as well as RIs for RV longitudinal strain (RVLS) values.[3,22,25,26] However, these studies used software designed for the LV.

No RIs for RV strain values using a dedicated RV software and using a comparably large sample size are available in dogs. Therefore, the first aim of our study was to determine the effect of body weight (BW), age, and heart rate (HR) on the RV indices TAPSE, TVI S′, FAC, right ventricular area in diastole (RVEDA), and systole (RVESA) and STE-derived RV global and free wall longitudinal strain as well as 3D TTE-derived RV diastolic (EDV) and systolic (ESV) volume and RV ejection fraction (EF).

Based on this information, the second aim was to generate reliable RIs of those indices by calculating prediction intervals (PIs).

2 | MATERIALS AND METHODS

The present multicenter study was designed as a prospective analysis. The study design was reviewed and approved by the Ethics Committee of the Ludwig-Maximilians-Universität München (permission number 190-05-11-2019).

2.1 | Animals

Privately owned dogs were presented to the Department of Veterinary Cardiology of the Ludwig-Maximilians-Universität München, Munich as well as to the Department of Veterinary Sciences of the University of Pisa and to the Anicura Istituto Veterinario Novara, for either routine cardiological assessment, breeding examination, or being recruited to participate in the study.

All dogs were determined to be healthy based on medical history, complete physical examination, cardiovascular examination, standard echocardiographic examination, and simultaneous electrocardiogram (ECG). Only dogs with a body condition score between 4 and 5 (out of 9) were included. Dogs were excluded if any arrhythmia other than sinus arrhythmia or a history of respiratory or cardiac disease were present. Other exclusion criteria were medications that affect cardiovascular system or abnormal findings on echocardiography including 2D, M-Mode, or Doppler findings. Dogs with trivial valvular regurgitation were not excluded if no abnormalities were detected in auscultation and the affected valve was morphologically normal.

2.2 | Conventional echocardiographic examination

Echocardiographic examination was performed by experienced board-certified cardiologists (G. Wess, O. Domenech) or residents under their direct supervision (T. Vezzosi, J. Eberhard, J. Friederich) using the following ultrasound units: Philips Epic 7, Vivid iq (GE Healthcare, Milano, Italy) and Aplio 300 (Canon Medical Systems Europe,

Zoetermeer, the Netherlands). Dogs were examined in right and left lateral recumbency without being sedated. An ECG was recorded simultaneously, and HR was monitored. Routine transthoracic 2D, M-Mode, and spectral and color flow Doppler echocardiography was undertaken as described.[27]

2.3 | Right ventricular systolic function

The left apical 4-chamber view was adapted for an optimized imaging of the RV.[15] Increased frame rates to improve image quality were reached by keeping the image sector narrow and decreasing depth. Right ventricular areas were determined by tracing the endocardial border from the parietal tricuspid annulus along the RV free wall to the apex and back to the septal tricuspid annulus along the interventricular septum at end-diastole (RVEDA) and end-systole (RVESA).[15] The percentage RV FAC was calculated using the formula: FAC (%) = (end-diastolic area − end-systolic area) ÷ end-diastolic area × 100.[15]

TAPSE was measured from a M-mode recording of the lateral aspect of the tricuspid valve annulus by aligning the M-Mode cursor parallel to the right ventricular free wall, showing the displacement of the tricuspid valve plane.[14]

Peak systolic annular velocity (S′) was measured using Pulsed-waved TDI velocities of longitudinal myocardial motion at the lateral tricuspid annulus. To avoid underestimation of velocity, the Doppler cursor was aligned as parallel as possible to the longitudinal plane of the RV free wall.[22]

Myocardial deformation measured by 2D speckle tracking is based on frame-by-frame tracking of small speckle patterns within the myocardial region of interest on grayscale echocardiographic images.[28]

Two-dimensional strain measurements were obtained from an apical 4-chamber view optimized for the right heart. Images from all centers were analyzed offline using TomTec software (RV 2D cardiac performance analysis, Image Arena, Munich, Germany). Frame rates from 73 to 117 Hz were achieved.

The RV endocardium was traced using several points starting from the parietal tricuspid valve annulus toward the apex and back to the septal one, beginning with end-systole and followed by end-diastole. The software analysis was performed automatically, but the contour was manually adapted where necessary to ensure adequate endocardial tracking. The RV free wall and septal wall were divided into 3 segments (basal, middle, and apical). Strain values were generated by the software for each of the segments as well as for global strain from the entire RV. Only strain curves of the endocardial layer were used. Global RVLS was calculated by averaging peak longitudinal strain measurements of the 6 segments and free wall RVLS was determined by averaging values of 3 RV free wall segments[6] (Figure 1).

2.4 | 3D TTE derived RV volume

The technical facilities for recording 3D images were only available at 1 center (LMU Munich). To generate 3D images, a X5-1 and X7-2 matrix probe was used. A single-beat examination was performed with frame rates from 29 to 77 Hz.

ECG was recorded simultaneously and the left-apical 4-chamber view was optimized for the RV as described above. Harmonic imaging technique was used. Imaging sector and elevation was kept as narrow as possible to optimize image quality.

Due to the requirement of the 3D software, it was necessary that at least half of the LV remained in the image section, since the LV is required for RV volume generation. Loops were recorded and RV volume was generated offline using TomTec software (4D RV-Function 2).

Several anatomic landmarks are required to calculate RV volumes: first, markers were placed at the LV apex and in the center of the mitral valve as well as at the RV apex and in the center of the tricuspid valve. Second, the aortic valve leaflets in the LV outflow tract and the RV in short axis were determined (Figure 2). Subsequently, the endocardial borders were tracked automatically by the software in long-axis as well as in short axis at basal, medial, and apical levels in end-systole and end-diastole followed by manual adjustment if necessary. A 3D dynamic RV model was generated. Inflow and outflow tract as well as papillary muscles and trabeculae were included in RV volume.[20,29] A complete RV volume was generated throughout the entire cardiac cycle, and end-diastolic volume (EDV), end-systolic volume (ESV), stroke volume (SV), and EF were determined as described.[30]

2.5 | Statistical analysis

Outliers were detected as described by Tukey's method,[31] categorizing outliers as "outside" and "far out" values. All observed outliers were visually inspected and only excluded if an error in measurement was found or if the image quality was too poor to generate reliable measurements.

We evaluated intraobserver and interobserver measurement variability with the coefficient of variation (CV), based on 9 randomly selected dogs. For intraobserver measurement variability, each RV variable of each selected dog was measured twice by 1 investigator. For interobserver measurement variability, each variable of each selected dog was measured by 2 different investigators (G. Wess and E.K. Feldhütter), blinded to each other's results.

For evaluating possible influences of age and HR on the RV variables, we estimated multiple linear regression models.[32] These "RV models" included BW as additional control variable, because many cardiac dimensions vary depending on size and BW of the dog. Visual inspection of the model errors showed no substantial deviation from the model assumptions.

The estimation of RIs is based on additional regression models where the RV variables are only dependent on some weight measure. As described, previous studies found approximate linear relations between (a) cardiac volumes and BW, (b) cross-sectional areas (eg, RVEDA and RVESA) and body surface area (BSA), and (c) cardiac linear dimensions (eg, TAPSE) and body length.[33] For every RV variable, all 3 relationships were evaluated and the most suitable one was chosen by visual comparison. Before model estimation, all RV variables were

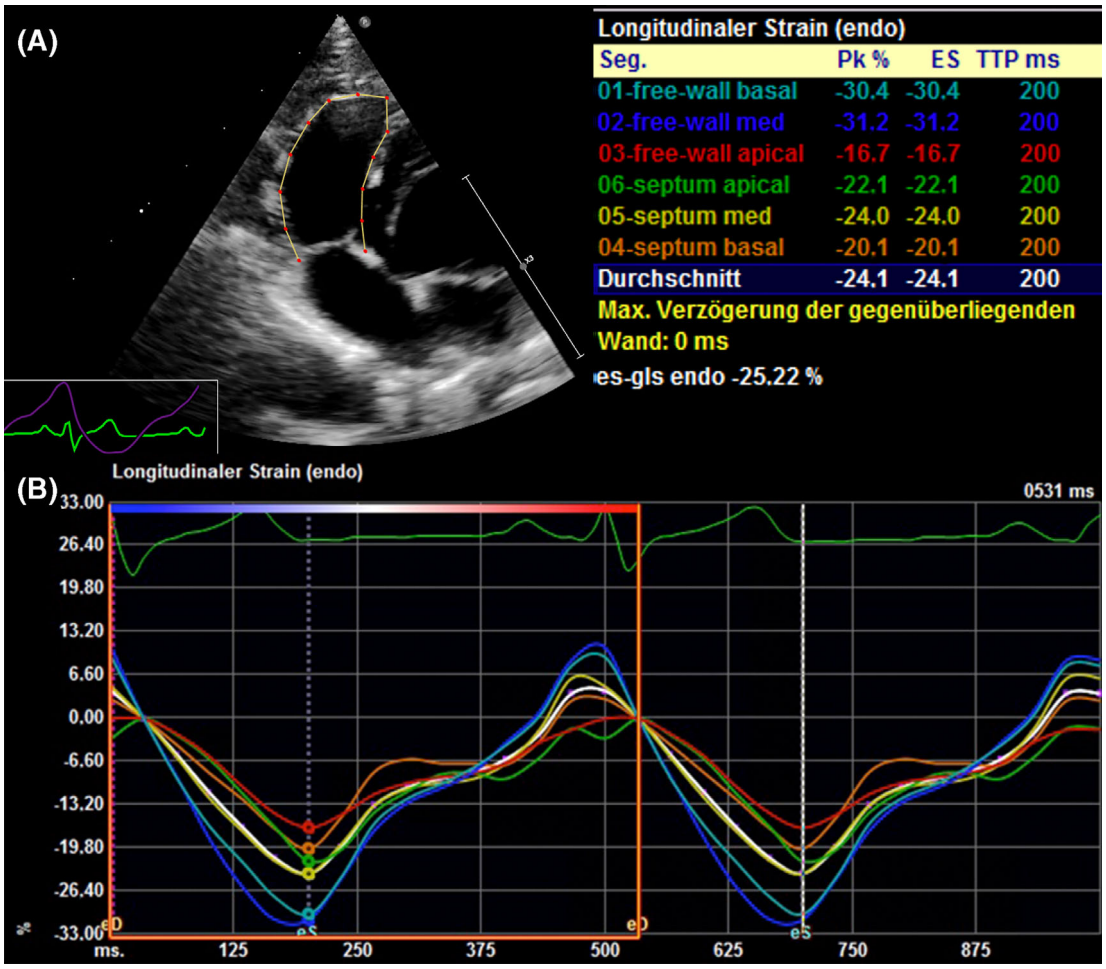

FIGURE 1 Illustration of strain measurement using STE. (A) Definition of the endocardial borders of the RV. (B) The software generates Strain curves of all 6 segments. Strain values are given as peak (PK), end-systolic (ES), and time to peak (TTP). RV, right ventricle; STE, speckle-tracking echocardiography

logarithmically transformed to achieve a more symmetric distribution. For the subsequent estimation of PIs based on the regression models, a back transformation was performed accordingly.

The regression equation is derived from the logarithmic form of the allometric equation and is of the form

$$\log(Y) = \log(c) + b\log(\mathrm{BW}) = a + b\log(\mathrm{BW})$$

where Y represents the RV variables, $c = \exp(a)$ the proportionality constant and b the scaling exponent.[33] To check the validity of this allometric scaling model, an additional additive regression model with a potentially nonlinear weight effect was estimated for each RV variable, based on a nonlinear effect with a P-spline representation,[32] as practiced in recent studies.[34] The linear and the additive model were then compared using a likelihood ratio test.[32]

If only a weak or no correlation with BW was found, weight-independent upper or lower limits are presented, by calculating right-sided (upper limit) or left-sided (lower limit) 95% RIs.[35] For weight-dependent variables, where allometric scaling was reasonable, the linear model was used to determine 95% PIs.[32] Additionally to those PIs, values for each RV index were normalized using the exponents calculated from the allometric scaling model. Subsequently, upper or lower limits, respectively, were determined for the normalized values as well.

The weight-independent and the additional limits for the regression models are estimated based on a nonparametric approach. If sample size is smaller than 120 subjects, a bootstrap approach is used as a robust method.[36,37] For a sample size of more than 120 subjects, the Clinical and Laboratory Standards Institute (CLSI) guidelines C28-A2 and C28-A3 for estimating percentiles and their 90% confidence intervals were followed.[35] Therefore, percentiles were calculated as the observations corresponding to rank $r = p^*(n + 1)$. For the 90% confidence intervals of the reference limits, the CLSI guidelines were followed as well and conservative confidence intervals were calculated using integer ranks.[35]

All analyses were performed using the commercially available software Medcalc (MedCalc, version 19.5.3, Ostend, Belgium), as well as the open-source software R (R Core Team 2020. R: A language and environment for statistical computing. R Foundation for Statistical Computing. URL: https://www.R-project.org, Vienna, Austria).

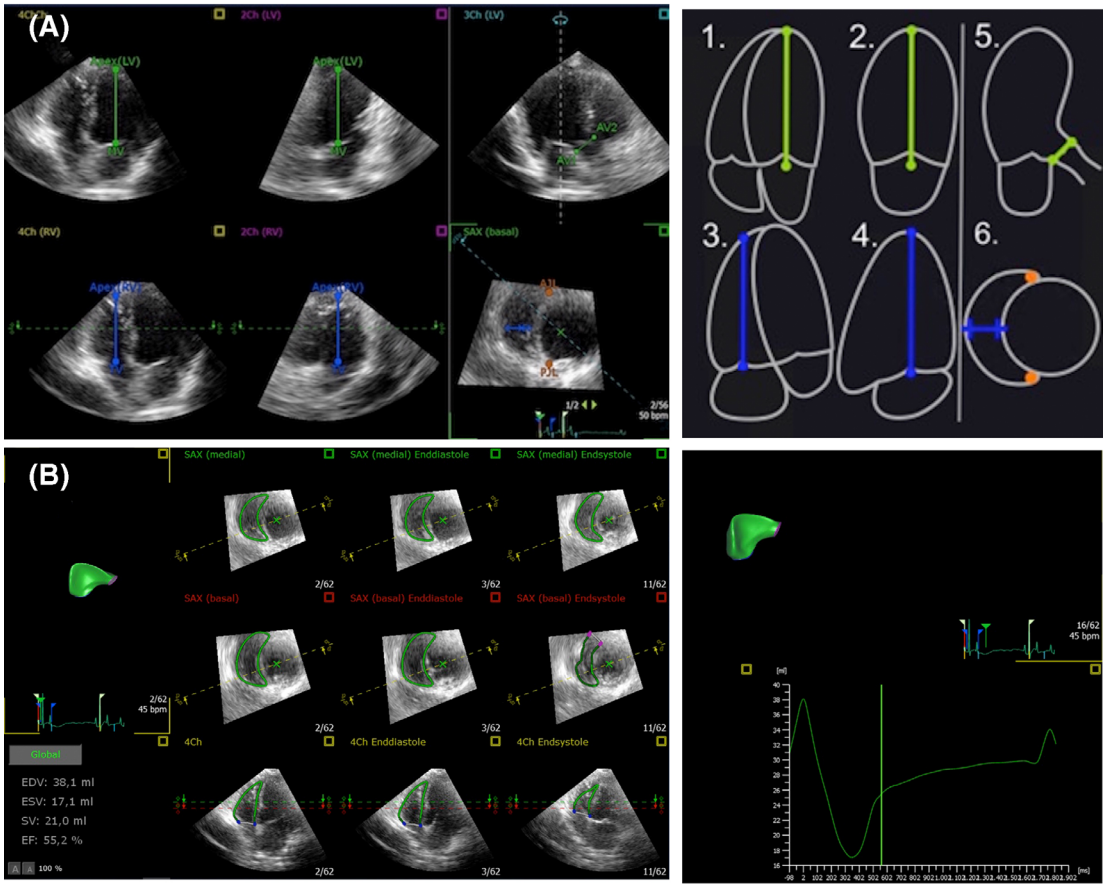

FIGURE 2 (A) Identification of anatomic landmarks in end-diastole in the left-apical 4-chamber view. Markers were placed as shown at the LV apex and in the center of the mitral valve as well as at the RV apex and in the center of the tricuspid valve. Followed by the landmarks of the short axis, aortic valve leaflets in the LV outflow tract were determined as well as the RV in short-axis. (B) Automatically tracing of the endocardial borders by the software in long-axis as well as in short axis at basal, medial, and apical levels in end-systole and end-diastole followed by manual adjustment if necessary. A 3D dynamic RV model including complete RV volume determination with EDV, ESV, SV, and EF is generate. EDV, end-diastolic volume; EF, ejection fraction; ESV, end-systolic volume; LV, left ventricle; RV, right ventricle; SV, stroke volume

Additive regression models in R were estimated with function "gam" from package "mgcv."[38] Linear models with function "lm" from package "stats." A *P* value of less than .05 was considered statistically significant.

3 | RESULTS

A total of 223 dogs were included from October 2014 until July 2020 and all of them were ≥12 months of age and consisted of heterogeneous breeds and BWs. Eleven dogs were excluded due to poor image quality. Two hundred and eleven dogs remained in the study, among which 59 breeds and mixed breeds were represented. The most represented breed were mixed breed (n = 44), followed by Labrador Retriever (n = 21), Golden Retriever (n = 16), Australian Shepherd (n = 13), Boxer (n = 9), Jack Russell Terrier (n = 8), Dachshund (n = 7), Chihuahua (n = 6), Yorkshire Terrier (n = 5), Border Collie (n = 5), Doberman Pincher (n = 4), French Bulldog (n = 4), Irish Wolfhound (n = 4), Vizsla (n = 3), White Swiss Shepherd Dog (n = 2), Weimaraner (n = 2), Shetland Sheepdog (n = 2), Rhodesian Ridgeback (n = 2), Pug (n = 2), Miniature Australian Shepherd (n = 2), Malinois dog (n = 2), Lagotto Romagnolo (n = 2), Labradoodle (n = 2), English Springer Spaniel (n = 2), English Bulldog (n = 2), Cocker Spaniel (n = 2), and 31 other breeds, each with 1 representative.

One hundred and twenty-six dogs were female and 86 dogs were male. The median age was 54 months (range, 12-169 months) and the median bodyweight 21.6 kg (range, 1.78-64.5 kg). The HR varied between 40 and 240 beats per minute (bpm) (median: 93 bpm). Trivial valvular regurgitation was observed by color Doppler imaging of the tricuspid valve (n = 3), the aortic valve (n = 1), the mitral valve (n = 3), and pulmonic valve (n = 1). Two dogs had a mildly accelerated aortic flow velocity observed by PW-Doppler with a maximal velocity of 1.9 m/s. 3D images (EDV, ESV, and EF) were taken of a total of 116 dogs, with EF ranging from 41.1% to 62.7%. Free wall RVLS strain was obtained in 206 dogs and values ranged from −17.93% to −51.56%. Global RVLS strain was obtained in 208 dogs and ranged from −14.6% to −46.18%. For area measurements (RVEDA, RVESA,

and FAC), a total of 211 dogs were evaluated and FAC ranged from 23.15% to 62.98%. For TAPSE and TVI S′ measurements, a total of 206 and 189 dogs, respectively, were included.

Intraobserver measurement variability was good for all variables with CV less than 10%. Interobserver measurement variability was also good with all variables showing a CV less than 10%, except FAC (CV = 11.2%) and ESV (CV = 11.2%).

FAC ($P < .01$) and TVI S′ ($P < .001$) correlated positively with HR, while RVEDA ($P < .001$) and RVESA ($P < .001$) showed a negative correlation with HR. All other variables did not show a significant correlation with HR. Only free wall RVLS ($P < .01$), EF ($P = .05$), and RVEDA ($P = .02$) displayed a mild negative correlation with age. All results of linear regression analysis are summarized in Table 1.

Some variables, including EF, FAC, free wall RVLS, and global RVLS, showed only a very weak or no relevant weight dependence. The remaining variables (TAPSE, TVI S′, EDV, ESV, RVEDA, RVESA) were weight-dependent. For those, the most suitable scaling parameter was determined by visual inspection of the scatter plots. As expected, TAPSE and TVI S′ correlated best with body length ($BW^{\frac{1}{3}}$), EDV, and ESV with bodyweight (in kg) and RVEDA and RVESA with BSA ($BW^{\frac{2}{3}}$).

In Figure 3, the comparison between the allometric scaling model and the additive model is displayed. Apparently, the allometric scaling model fits better for every investigated variable. Results of linear regression analysis of allometric scaling are shown in Table 2. Subsequently, PIs related to BW for EDV, ESV, TAPSE, RVEDA, RVESA, and TVI S′ were calculated and summarized in Table 3. The following upper limits were generated for normalized variables: A value of EDVn ≤2.5 $mL/kg^{0.942}$, ESVn ≤1.2 $mL/kg^{0.962}$, TAPSEn ≥4.5 $mm/kg^{0.285}$, RVEDAn ≤1.4 $cm^2/kg^{0.665}$, RVESAn ≤0.8 $cm^2/kg^{0.695}$, and TVI S′n ≥5.6 $cm/s/kg^{0.186}$ were considered normal.

The scatter plot in Figure 4 displays the 95% PIs and the regression line of selected variables normalized to BW using the corresponding scaling exponent.

For all other variables, which are widely weight-independent, upper or lower limits were generated. For EF and FAC, values above 42.1% and 30.0% were considered normal, respectively. In terms of strain, values lower (ie, more negative) than −20.8% for free wall and −18.3% for global RVLS were considered normal.

To verify our results, we subsequently calculated how many dogs were under or above the calculated lower or upper limits for each variable: regarding the volumetric measurements, in EDVn fell 5 out of 116 dogs (4.3%) and in ESVn 7 dogs (6.0%) above the upper limit. In EF fell 6 dogs (5.2%) under the lower limit. In case of the area measurements, 9 out of 211 dogs (4.3%) were above the upper limit at RVEDAn, 11 dogs (5.2%) at RVESAn and 16 dogs (7.6%) under the lower limit at FAC. Ten dogs out of 206 and 189 (4.8% and 5.3%) showed lower TAPSEn and TVI S′n values, respectively, than the calculated lower limits are. Looking at 2D strain, 12 out of 206 dogs (5.8%) and 13 out of 208 dogs (6.2%) had decreased strain values in free wall and global RVLS, respectively.

4 | DISCUSSION

This study generates reference values for global and free wall right ventricular strain and RV 3D volume using a software that is especially designed for the RV. The number of dogs involved is larger than in previous studies.[22,25] As the RV becomes increasingly important in clinical evaluation of dogs with heart disease, it is currently more necessary to have reliable reference values available.

All variables showed a good repeatability, but only inter- and intraobserver measurement variability was evaluated in this study. This reflects only 1 component of variability what needs to be considered when thinking of variability and repeatability of these variables. As with all echocardiographic measurements, the quality depends largely on the experience and competence of the investigator. The echocardiographic examination should therefore be performed by a

TABLE 1 Correlation coefficients derived by multiple linear regression analyses

	Bodyweight		Age		Heart rate	
	Partial correlation	*P* value	Partial correlation	*P* value	Partial correlation	*P* value
EDV	0.92	<.001	−0.16	.08	0.02	.81
ESV	0.91	<.001	−0.10	.03	0.05	.6
EF	−0.18	.5	−0.18	.05	0.01	.93
Free wall RVLS	0.12	.1	0.16	.03	−0.09	.19
Global RVLS	0.12	.1	0.12	.08	−0.06	.37
TAPSE	0.65	<.001	−0.01	.97	0.08	.24
RVEDA	0.88	<.001	−0.16	.02	−0.25	<.001
RVESA	0.84	<.001	−0.07	.35	−0.25	<.001
FAC	−0.29	.04	−0.03	.86	0.39	.01
TVI S′	0.45	<.001	0.07	.33	0.28	<.001

Abbreviations: EDV, 3D RV end-diastolic volume; EF, ejection fraction; ESV, 3D end-systolic volume; FAC, fractional area change; Free wall RVLS, free wall RV longitudinal strain; Global RVLS, global RV longitudinal strain; RVEDA, RV end-diastolic area; RVESA, RV end-systolic area; TAPSE, tricuspid annular plane systolic excursion; TVI S′, tissue Doppler imaging-derived systolic myocardial velocity of the lateral tricuspid annulus.

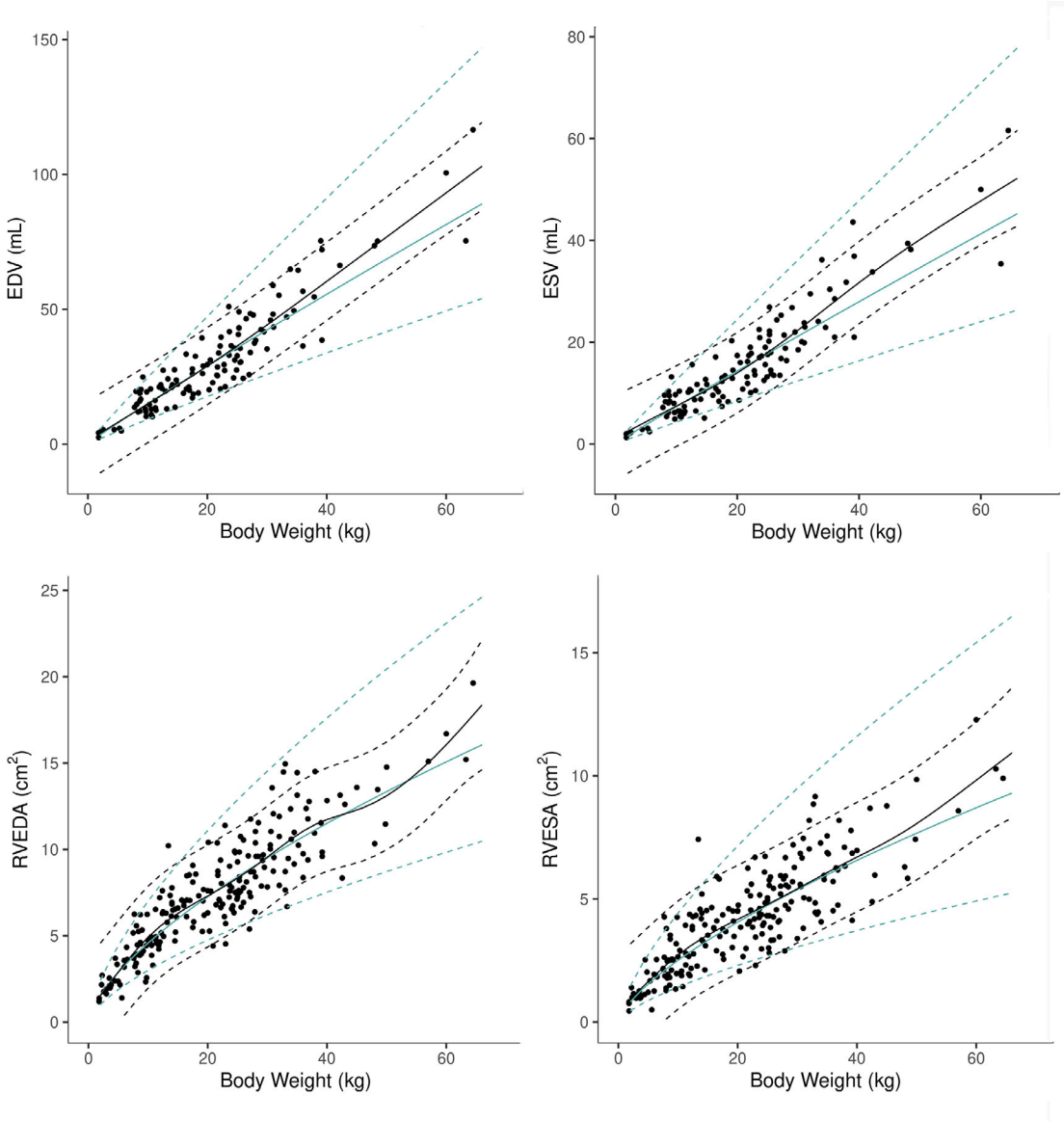

FIGURE 3 Comparison of the linear regression (blue lines) and the additive model (black lines) for each RV function index. Upper and lower prediction intervals and the means are displayed as dashed and solid lines, respectively. RV, right ventricle

well-trained cardiologist. Only FAC and ESV had CV higher than 10%. The sometimes poorly traceable endocardial borders in systole could explain the relatively low repeatability of ESV. This fact emphasizes once again how important a high image quality is for the generation of 3D loops.

Acquiring 3D volumes of the RV includes the entire RV, including inflow, outflow, and apical region, without being dependent on geometric assumptions. Therefore, it can be an important index for RV assessment in diseases that lead to RV volume or pressure overload or systolic dysfunction, such as PH.[5-7] The reduction in RV systolic function in dogs with PH might result in consequences for treatment or life expectancy. Also in dogs with myxomatous mitral valve disease, the RV function indices might serve as additional prognostic factors.[1] In human patients with arrhythmogenic right ventricular cardiomyopathy (ARVC), RV free wall strain reduction is associated with structural disease progression and therefore with treatment and follow-up decisions.[39] In people with dilated cardiomyopathy (DCM), RV dysfunction results in poor clinical outcome.[40] Therefore, it is of clinical importance to be able to accurately determine the function and size of the RV.

Due to its special geometry, 3D images are particularly important for correct assessment of the RV. Echocardiographic methods used to calculate LV volumes, such as the Simpson's Method of Disks (SMOD) exclude the RV outflow tract and are therefore not recommended during routine assessment of the RV in humans.[15]

Two-dimensional or "speckle tracking" strain is a newer method that allows tissue tracking to occur in 2 dimensions. It allows global and regional strain to be measured using frame by frame tracking of

TABLE 2 Results of linear regression analysis of allometric scaling using the formula: log10_Variable = $a + b$ * log10_BW

RV function index	*a*	*b*	R^2
RVEDA	−0.004	0.665	0.839
RVESA	−0.296	0.695	0.761
TAPSE	0.790	0.285	0.521
EDV	0.235	0.942	0.866
ESV	−0.095	0.962	0.852
TVI S′	−1.076	0.186	0.216

Note: *a*: constant, *b*: scaling exponent, and R^2: coefficient of determination.
Abbreviations: EDV, 3D RV end-diastolic volume; ESV, 3D end-systolic volume; RV, right ventricle; RVEDA, RV end-diastolic area; RVESA, RV end-systolic area; TAPSE, tricuspid annular plane systolic excursion; TVI S′, tissue Doppler imaging-derived systolic myocardial velocity of the lateral tricuspid annulus.

unique "speckles" within the myocardium produced by interference between scattered ultrasound waves. Free wall RVLS values were higher than global RVLS, which is consistent with other studies.[3,41] In humans, it is recommended to only use free wall RVLS as a default variable.[42] Although the ventricular septum contributes substantially to RV systolic function, it remains primarily a part of the LV.[42] Since some studies proved that free wall RVLS correlated better with RV EF obtained by MRI than global RVLS,[41] it might also be advisable in dogs to use the RV free wall for RVLS measurements for the assessment of systolic function of the RV. We evaluated only longitudinal strain measurements because the longitudinal axis seems to accurately reflect the global contractile function of the RV.[43] In general, a distinction can also be made between endocardial myocardial and epicardial strain measurements, related to the different layers of the cardiac walls. For several reasons, we took only endocardial strain measurements into consideration. First, there were practical reasons for this: the endocardial layer of the RV is the best to visualize and therefore most accurate to determine and follow over the cardiac cycle. Second, the RV differs from the LV in its wall structure: while the wall of the LV includes 3 layers, the RV consists only of 2 layers, the superficial (subepicardial) and the deep (subendocardial) layer.[44] The fibers of the superficial layer are arranged circumferentially and the fibers of the subendocardial layer are longitudinally aligned from base to apex. Additionally, the subendocardial layer contributes about 80% to the RV contraction.[41,44] In human medicine deformation of the endocardial layer is more important than in the other layers and that the level of endocardial strain detection by the software is probably the most important factor.[45] Therefore, longitudinal strain of the endocardial layer should accurately represent RV systolic function.

Technically, the endocardial layer is also the most suitable one to track and follow over the cardiac cycle.

In contrast to other studies, we observed no relationship between BW and strain measurements.[3,22] The calculated normal values of −20.8% for free wall and −18.3% for global RVLS are comparable to other studies in humans.[46] Also in dogs, similar results have been found in the past: normal strain values of −19.0% ± 3.1 for free wall RVLS and −15.3% ± 2.7 for global RVLS have been published.[3] In another study, strain was normalized to BW and normal values between −20.2% and −24.7% for free wall RVLS were received.[22] It might be important that more negative strain value reflects better systolic function.

For EF, values above 42.1% were considered normal. This value is close to the normal value in human medicine, which is 45% for EF.[16] The lower normal value of 30% for FAC measurements is comparable with the results of other studies, where 41% ± 8[3] or 32% to 69%[22] were stated normal. In those studies, FAC was normalized to BW. Due to the very weak correlation and the visual inspection of the scatter plot, we decided against normalization in the present study. Our calculated normal value is comparable to human medicine, where it is also reported to be 35%.[16] The values of FAC measurements show a relatively high variance. This could be explained by easily occurring measurement deviations followed by differences in FAC values up to 5% to 15%.

For all other variables, weight-dependent PIs using allometric scaling were calculated and are shown in Table 3. Without calculations, cardiologists can quickly find out whether the dog is within the reference range.

This regression model is a widely accepted procedure in order to create reference values in dogs.[33,34] The regression model was more accurate than the additive model, because the latter model calculated especially in the lower weight segments too wide ranges of PIs, which could lead to false or inaccurate estimations in small dogs. However, the PIs must be interpreted with caution in larger dogs approximately >40 kg, since comparatively few dogs were included, and the regression model has therefore a wide range of normal PIs.

Additionally, upper respectively lower limits for normalized indices to bodyweight using the corresponding exponent were proposed. Cardiologists can therefore decide which approach to use.

Heart rate correlated positively with FAC and TVI S′, while a negative correlation was found between HR and RVEDA and RVESA. This observation should be considered in dogs with high or low HRs.

Area measurements such as RVEDA correlated best with BSA and that is consistent with results from previous studies.[5,47] Vezzosi et al therefore proposed the RVEDA index, as already used in human medicine.[5]

In order to obtain accurate measurements, it is very important to avoid foreshortening of the RV, as this can lead to incorrect measurements. Therefore, a modified apical 4-chamber view optimized for the RV should be used, if right heart disease is suspected.

There are several limitations of the present study. First, there is no follow-up available of the examined dogs and no blood pressure measurements were performed. Therefore, it cannot be excluded that the dogs will develop heart disease during their lifetime. Second, although a comparatively large number of dogs was included to generate the PIs in the present study, an even larger number would certainly provide a higher representation of the broader dog population, especially at the upper and lower edges of the weight ranges. The

TABLE 3 95% prediction intervals for EDV, ESV, TAPSE, RVEDA, RVESA, and TVI S′ of the right ventricle for dogs of varying weights

Body weight (kg)	EDV (mL)	ESV (mL)	TAPSE (mm)	RVEDA (cm^2)	RVESA (cm^2)	TVI S′ (m/s)
2	3.3 (1.97-5.53)	1.57 (0.9-2.73)	7.51 (5.03-11.22)	1.57 (1.02-2.42)	0.82 (0.46-1.46)	9.54 (5.67-16.05)
4	6.35 (3.84-10.5)	3.05 (1.77-5.26)	9.15 (6.15-13.6)	2.49 (1.62-3.82)	1.33 (0.75-2.35)	10.85 (6.49-18.14)
6	9.3 (5.65-15.31)	4.5 (2.63-7.72)	10.27 (6.91-15.24)	3.26 (2.13-5)	1.76 (0.99-3.11)	11.7 (7.01-19.51)
8	12.2 (7.43-20.03)	5.94 (3.47-10.16)	11.14 (7.51-16.52)	3.95 (2.58-6.04)	2.15 (1.21-3.79)	12.34 (7.41-20.55)
10	15.05 (9.18-24.68)	7.36 (4.31-12.57)	11.87 (8.01-17.6)	4.58 (3-7)	2.51 (1.42-4.42)	12.86 (7.73-21.4)
12	17.87 (10.91-29.28)	8.78 (5.14-14.97)	12.5 (8.44-18.53)	5.17 (3.38-7.9)	2.84 (1.61-5.02)	13.3 (8-22.13)
14	20.67 (12.62-33.84)	10.18 (5.97-17.36)	13.06 (8.82-19.36)	5.73 (3.75-8.76)	3.17 (1.79-5.58)	13.69 (8.23-22.77)
16	23.44 (14.32-38.37)	11.58 (6.79-19.73)	13.57 (9.16-20.11)	6.26 (4.1-9.57)	3.47 (1.97-6.13)	14.04 (8.44-23.34)
18	26.19 (16-42.87)	12.96 (7.61-22.1)	14.03 (9.47-20.79)	6.77 (4.43-10.35)	3.77 (2.14-6.65)	14.35 (8.63-23.86)
20	28.92 (17.67-47.35)	14.35 (8.42-24.46)	14.46 (9.76-21.43)	7.26 (4.75-11.1)	4.06 (2.3-7.15)	14.63 (8.8-24.33)
22	31.64 (19.33-51.8)	15.73 (9.22-26.81)	14.86 (10.03-22.02)	7.74 (5.06-11.82)	4.33 (2.46-7.64)	14.89 (8.95-24.77)
24	34.35 (20.98-56.24)	17.1 (10.03-29.16)	15.23 (10.28-22.57)	8.2 (5.36-12.53)	4.6 (2.61-8.12)	15.13 (9.1-25.17)
26	37.04 (22.61-60.66)	18.47 (10.83-31.5)	15.58 (10.51-23.09)	8.65 (5.66-13.22)	4.87 (2.76-8.59)	15.36 (9.23-25.55)
28	39.72 (24.24-65.07)	19.83 (11.62-33.84)	15.91 (10.73-23.59)	9.08 (5.94-13.88)	5.12 (2.9-9.04)	15.57 (9.36-25.91)
30	42.38 (25.86-69.46)	21.19 (12.42-36.18)	16.23 (10.95-24.06)	9.51 (6.22-14.54)	5.38 (3.05-9.49)	15.77 (9.48-26.25)
32	45.04 (27.47-73.84)	22.55 (13.21-38.51)	16.53 (11.15-24.51)	9.93 (6.49-15.18)	5.62 (3.19-9.93)	15.96 (9.59-26.57)
34	47.69 (29.08-78.21)	23.91 (14-40.84)	16.82 (11.34-24.94)	10.33 (6.76-15.8)	5.86 (3.32-10.36)	16.14 (9.7-26.88)
36	50.33 (30.68-82.57)	25.26 (14.78-43.17)	17.09 (11.52-25.35)	10.73 (7.02-16.42)	6.1 (3.46-10.78)	16.32 (9.8-27.17)
38	52.96 (32.27-86.92)	26.61 (15.56-45.49)	17.36 (11.7-25.75)	11.13 (7.27-17.02)	6.34 (3.59-11.19)	16.48 (9.89-27.45)
40	55.58 (33.85-91.25)	27.95 (16.34-47.81)	17.61 (11.87-26.13)	11.51 (7.52-17.62)	6.57 (3.72-11.6)	16.64 (9.99-27.72)
42	58.2 (35.43-95.58)	29.3 (17.12-50.13)	17.86 (12.03-26.5)	11.89 (7.77-18.2)	6.79 (3.84-12)	16.79 (10.08-27.98)
44	60.8 (37.01-99.91)	30.64 (17.9-52.45)	18.1 (12.19-26.86)	12.27 (8.01-18.77)	7.02 (3.97-12.4)	16.94 (10.16-28.23)
46	63.4 (38.57-104.22)	31.98 (18.67-54.76)	18.33 (12.35-27.21)	12.63 (8.25-19.34)	7.24 (4.09-12.79)	17.08 (10.24-28.47)
48	66 (40.14-108.53)	33.31 (19.45-57.07)	18.55 (12.49-27.54)	13 (8.49-19.9)	7.45 (4.21-13.18)	17.21 (10.32-28.7)
50	68.59 (41.69-112.83)	34.65 (20.22-59.39)	18.77 (12.64-27.87)	13.35 (8.72-20.45)	7.67 (4.34-13.56)	17.34 (10.4-28.93)
52	71.17 (43.25-117.12)	35.98 (20.99-61.7)	18.98 (12.78-28.19)	13.71 (8.95-20.99)	7.88 (4.45-13.94)	17.47 (10.47-29.15)
54	73.75 (44.8-121.4)	37.31 (21.75-64)	19.18 (12.91-28.49)	14.05 (9.18-21.53)	8.09 (4.57-14.31)	17.59 (10.54-29.36)
56	76.32 (46.34-125.69)	38.64 (22.52-66.31)	19.38 (13.05-28.8)	14.4 (9.4-22.06)	8.3 (4.69-14.68)	17.71 (10.61-29.56)
58	78.88 (47.88-129.96)	39.97 (23.28-68.62)	19.58 (13.18-29.09)	14.74 (9.62-22.58)	8.5 (4.8-15.05)	17.83 (10.68-29.76)
60	81.44 (49.42-134.23)	41.29 (24.04-70.92)	19.77 (13.3-29.38)	15.07 (9.84-23.1)	8.7 (4.92-15.41)	17.94 (10.74-29.96)
62	84 (50.95-138.49)	42.62 (24.8-73.22)	19.95 (13.42-29.66)	15.41 (10.05-23.61)	8.9 (5.03-15.77)	18.05 (10.81-30.15)
64	86.55 (52.47-142.75)	43.94 (25.56-75.53)	20.13 (13.54-29.93)	15.73 (10.26-24.12)	9.1 (5.14-16.12)	18.16 (10.87-30.33)
66	89.1 (54-147.01)	45.26 (26.32-77.83)	20.31 (13.66-30.2)	16.06 (10.48-24.62)	9.3 (5.25-16.48)	18.26 (10.93-30.51)

Abbreviations: EDV, 3D RV end-diastolic volume; ESV, 3D end-systolic volume; RV, right ventricle; RVEDA, RV end-diastolic area; RVESA, RV end-systolic area; TAPSE, tricuspid annular plane systolic excursion; TVI S′, tissue Doppler imaging-derived systolic myocardial velocity of the lateral tricuspid annulus.

number of dogs used for 3D images was lower, as only 1 of our study centers had the equipment to acquire 3D images.

Third, the reference values generated with this particular software can only be compared to a limited extent to values of any other software and should not be used interchangeable. This primarily concerns strain and 3D volumes.

Even though 3D echocardiography seems to be a promising imaging method, it is not yet routinely used in veterinary medicine due to the requirement of special transducers and software. Furthermore, 3D imaging offers only a limited temporal resolution. Especially when it comes to higher HRs, the frame rate reduces image resolution. This fact might be a problem in particular for smaller dogs with very high HRs. Another point is the susceptibility to interference with 3D echocardiography. Moving or panting of the dog can possibly result in poor spatial resolution and stitching artifacts.[20]

Further studies are needed to possibly use 3D volume and strain additionally to other variables for treatment decisions or as

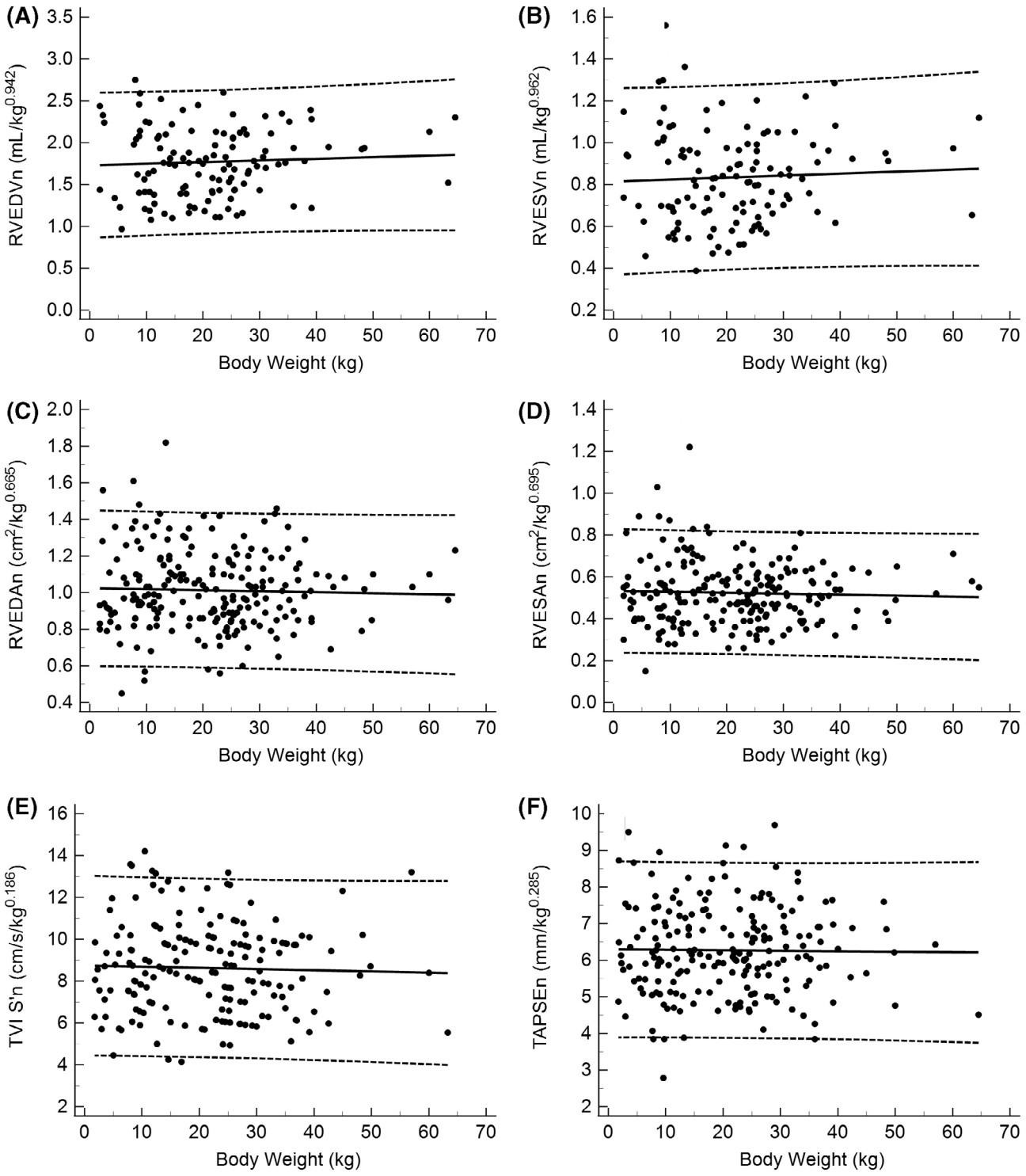

FIGURE 4 Scatter Plots and regression line (middle line) of the normalized RV indices using the calculated exponents. 95% prediction intervals are displayed (upper and lower lines). (A) End-diastolic volume normalized (EDVn); (B) End-systolic volume normalized (ESVn); (C) End-diastolic area normalized (EDAn); (D) End-systolic area normalized (ESAn); (E) Peak systolic tissue velocity normalized (TVI S′n); (F) Tricuspid annular plane systolic excursion normalized (TAPSEn). RV, right ventricle

prognostic factors for various diseases. Also, we did not include every RV function variable. Additional variables, such as right ventricular outflow tract fractional shortening, are useful when evaluating RV function.[48]

Some breeds, such as sighthounds or Doberman Pinschers, require their own breed-specific reference values for LV indices and it should be evaluated if breed specific PIs are also necessary for the RV.[34,49-53]

ACKNOWLEDGMENT

No funding was received for this study.

CONFLICT OF INTEREST DECLARATION

Authors declare no conflict of interest.

OFF-LABEL ANTIMICROBIAL DECLARATION

Authors declare no off-label use of antimicrobials.

INSTITUTIONAL ANIMAL CARE AND USE COMMITTEE (IACUC) OR OTHER APPROVAL DECLARATION

Approved by LMU Munich for all centers involved, number: 190-05-11-2019.

HUMAN ETHICS APPROVAL DECLARATION

Authors declare human ethics approval was not needed for this study.

ORCID

Tommaso Vezzosi https://orcid.org/0000-0001-8301-6582
Rosalba Tognetti https://orcid.org/0000-0001-8449-9176
Gerhard Wess https://orcid.org/0000-0002-6634-8072

REFERENCES

1. Chapel EH, Scansen BA, Schober KE, et al. Echocardiographic estimates of right ventricular systolic function in dogs with myxomatous mitral valve disease. *J Vet Intern Med*. 2018;32:64-71.
2. Le Tourneau T, Deswarte G, Lamblin N, et al. Right ventricular systolic function in organic mitral regurgitation: impact of biventricular impairment. *Circulation*. 2013;127:1597-1608.
3. Morita T, Nakamura K, Osuga T, et al. The repeatability and characteristics of right ventricular longitudinal strain imaging by speckle-tracking echocardiography in healthy dogs. *J Vet Cardiol*. 2017;19:351-362.
4. Saguner AM, Vecchiati A, Baldinger SH, et al. Different prognostic value of functional right ventricular parameters in arrhythmogenic right ventricular cardiomyopathy/dysplasia. *Circ Cardiovasc Imaging*. 2014;7:230-239.
5. Vezzosi T, Domenech O, Costa G. Echocardiographic evaluation of the right ventricular dimension and systolic function in dogs with pulmonary hypertension. *J Vet Intern Med*. 2018;32(5):1548-1548.
6. Morita T, Nakamura K, Osuga T, et al. Right ventricular function and dyssynchrony measured by echocardiography in dogs with precapillary pulmonary hypertension. *J Vet Cardiol*. 2019;23:1-14.
7. Visser LC, Wood JE, Johnson LR. Survival characteristics and prognostic importance of echocardiographic measurements of right heart size and function in dogs with pulmonary hypertension. *J Vet Intern Med*. 2020;34:1379-1388.
8. Sheehan F, Redington A. The right ventricle: anatomy, physiology and clinical imaging. *Heart*. 2008;94:1510-1515.
9. Haddad F, Hunt SA, Rosenthal DN, et al. Right ventricular function in cardiovascular disease, part I: anatomy, physiology, aging, and functional assessment of the right ventricle. *Circulation*. 2008;117:1436-1448.
10. Jenkins C, Chan J, Bricknell K, et al. Reproducibility of right ventricular volumes and ejection fraction using real-time three-dimensional echocardiography: comparison with cardiac MRI. *Chest*. 2007;131:1844-1851.
11. Caputo GR, Tscholakoff D, Sechtem U, et al. Measurement of canine left ventricular mass by using MR imaging. *AJR Am J Roentgenol*. 1987;148:33-38.
12. Markiewicz W, Sechtem U, Kirby R, et al. Measurement of ventricular volumes in the dog by nuclear magnetic resonance imaging. *J Am Coll Cardiol*. 1987;10:170-177.
13. Fries RC, Gordon SG, Saunders AB, et al. Quantitative assessment of two- and three-dimensional transthoracic and two-dimensional transesophageal echocardiography, computed tomography, and magnetic resonance imaging in normal canine hearts. *J Vet Cardiol*. 2019;21:79-92.
14. Pariaut R, Saelinger C, Strickland KN, et al. Tricuspid annular plane systolic excursion (TAPSE) in dogs: reference values and impact of pulmonary hypertension. *J Vet Intern Med*. 2012;26:1148-1154.
15. Rudski LG, Lai WW, Afilalo J, et al. Guidelines for the echocardiographic assessment of the right heart in adults: a report from the American Society of Echocardiography: endorsed by the European Association of Echocardiography, a registered branch of the European Society of Cardiology, and the Canadian Society of Echocardiography. *J Am Soc Echocardiogr*. 2010;23:685-713.
16. Lang RM, Badano LP, Mor-Avi V. Recommendations for cardiac chamber quantification by echocardiography in adults: an update from the American Society of Echocardiography and the European Association of Cardiovascular Imaging. *Eur Heart J Cardiovasc Imaging*. 2015;16:233-271.
17. Voigt J-U, Pedrizzetti G, Lysyansky P, et al. Definitions for a common standard for 2D speckle tracking echocardiography: consensus document of the EACVI/ASE/Industry Task Force to standardize deformation imaging. *J Am Soc Echocardiogr*. 2015;28:183-193.
18. Gopal AS, Chukwu EO, Iwuchukwu CJ, et al. Normal values of right ventricular size and function by real-time 3-dimensional echocardiography: comparison with cardiac magnetic resonance imaging. *J Am Soc Echocardiogr*. 2007;20:445-455.
19. van der Zwaan HB, Geleijnse ML, McGhie JS, et al. Right ventricular quantification in clinical practice: two-dimensional vs. three-dimensional echocardiography compared with cardiac magnetic resonance imaging. *Eur J Echocardiogr*. 2011;12:656-664.
20. Sieslack AK, Dziallas P, Nolte I, et al. Quantification of right ventricular volume in dogs: a comparative study between three-dimensional echocardiography and computed tomography with the reference method magnetic resonance imaging. *BMC Vet Res*. 2014;10:242.
21. Mondillo S, Galderisi M, Mele D, et al. Speckle-tracking echocardiography: a new technique for assessing myocardial function. *J Ultrasound Med*. 2011;30:71-83.
22. Visser LC, Scansen BA, Schober KE, et al. Echocardiographic assessment of right ventricular systolic function in conscious healthy dogs: repeatability and reference intervals. *J Vet Cardiol*. 2015;17:83-96.
23. Visser LC, Sintov DJ, Oldach MS. Evaluation of tricuspid annular plane systolic excursion measured by two-dimensional echocardiography in healthy dogs: repeatability, reference intervals, and comparison with M-mode assessment. *J Vet Cardiol*. 2018;20:165-174.
24. Caivano D, Rishniw M, Birettoni F, et al. Transverse right ventricle strain and strain rate assessed by 2-dimensional speckle tracking echocardiography in dogs with pulmonary hypertension. *Vet Sci*. 2020;7:19.
25. Chetboul V, Damoiseaux C, Lefebvre HP, et al. Quantitative assessment of systolic and diastolic right ventricular function by echocardiography and speckle-tracking imaging: a prospective study in 104 dogs. *J Vet Sci*. 2018;19:683-692.
26. Locatelli C, Spalla I, Zanaboni AM, et al. Assessment of right ventricular function by feature-tracking echocardiography in conscious healthy dogs. *Res Vet Sci*. 2016;105:103-110.
27. Thomas WP, Gaber CE, Jacobs GJ, et al. Recommendations for standards in transthoracic two-dimensional echocardiography in the dog and cat. *J Vet Intern Med*. 1993;7:247-252.
28. Kalogeropoulos AP, Georgiopoulou VV, Howell S, et al. Evaluation of right intraventricular dyssynchrony by two-dimensional strain

echocardiography in patients with pulmonary arterial hypertension. *J Am Soc Echocardiogr*. 2008;21:1028-1034.
29. Tamborini G, Marsan NA, Gripari P, et al. Reference values for right ventricular volumes and ejection fraction with real-time three-dimensional echocardiography: evaluation in a large series of normal subjects. *J Am Soc Echocardiogr*. 2010;23:109-115.
30. Genovese D, Rashedi N, Weinert L, et al. Machine learning-based three-dimensional echocardiographic quantification of right ventricular size and function: validation against cardiac magnetic resonance. *J Am Soc Echocardiogr*. 2019;32:969-977.
31. Tukey BH, John W. Exploratory data analysis. Addison-Wesley Publishing Company Reading, Mass. — Menlo Park, Cal., London, Amsterdam, Don Mills, Ontario, Sydney 1977, XVI, 688 S. *Biom J*. 1981;23:413-414.
32. Fahrmeir L, Kneib T, Lang S. *Regression: Models, Methods and Applications*. Heidelberg, Germany: Springer Science & Business Media; 2013.
33. Cornell C, Kittleson M, Torre P, et al. Allometric scaling of M-mode cardiac measurements in normal adult dogs. *J Vet Intern Med*. 2004; 18:311-321.
34. Esser LC, Borkovec M, Bauer A, et al. Left ventricular M-mode prediction intervals in 7651 dogs: population-wide and selected breed-specific values. *J Vet Intern Med*. 2020;34(6):2242-2252.
35. CLSI and IFCC. *C28-A3 document; Defining*. establishing and verifying reference intervals in the clinical laboratory: approved guideline-third edition; 2008;28:1-76.
36. Efron B, Tibshirani RJ. *An Introduction to the Bootstrap*. London: Taylor & Francis; 1994.
37. Friedrichs KR, Harr KE, Freeman KP, et al. ASVCP reference interval guidelines: determination of de novo reference intervals in veterinary species and other related topics. *Vet Clin Pathol*. 2012;41:441-453.
38. Wood SN. *Generalized Additive Models: An Introduction with R*. 2nd ed. London: CRC Press; 2017.
39. Malik N, Win S, James CA, et al. Right ventricular strain predicts structural disease progression in patients with arrhythmogenic right ventricular cardiomyopathy. *J Am Heart Assoc*. 2020;9:e015016.
40. Schalla S, Jaarsma C, Bekkers SC, et al. Right ventricular function in dilated cardiomyopathy and ischemic heart disease: assessment with non-invasive imaging. *Neth Heart J*. 2015;23:232-240.
41. Lee J-H, Park J-H. Strain analysis of the right ventricle using two-dimensional echocardiography. *J Cardiovasc Imaging*. 2018;26: 111-124.
42. Badano LP, Kolias TJ, Muraru D, et al. Standardization of left atrial, right ventricular, and right atrial deformation imaging using two-dimensional speckle tracking echocardiography: a consensus document of the EACVI/ASE/Industry Task Force to standardize deformation imaging. *Eur Heart J Cardiovasc Imaging*. 2018;19:591-600.
43. Leather HA, Ama' R, Missant C, et al. Longitudinal but not circumferential deformation reflects global contractile function in the right ventricle with open pericardium. *Am J Physiol Heart Circ Physiol*. 2006; 290:H2369-H2375.
44. Ho SY, Nihoyannopoulos P. Anatomy, echocardiography, and normal right ventricular dimensions. *Heart*. 2006;92(suppl 1):i2-i13.
45. Amzulescu MS, De Craene M, Langet H, et al. Myocardial strain imaging: review of general principles, validation, and sources of discrepancies. *Eur Heart J Cardiovasc Imaging*. 2019;20:605-619.
46. Jones N, Burns AT, Prior DL. Echocardiographic assessment of the right ventricle-state of the art. *Heart Lung Circ*. 2019;28:1339-1350.
47. Gentile-Solomon JM, Abbott JA. Conventional echocardiographic assessment of the canine right heart: reference intervals and repeatability. *J Vet Cardiol*. 2016;18:234-247.
48. Caivano D, Rishniw M, Birettoni F, et al. Right ventricular outflow tract fractional shortening: an echocardiographic index of right ventricular systolic function in dogs with pulmonary hypertension. *J Vet Cardiol*. 2018;20:354-363.
49. Wess G, Mäurer J, Simak J, et al. Use of Simpson's method of disc to detect early echocardiographic changes in Doberman Pinschers with dilated cardiomyopathy. *J Vet Intern Med*. 2010;24:1069-1076.
50. della Torre PK, Kirby AC, Church DB, et al. Echocardiographic measurements in greyhounds, whippets and Italian greyhounds—dogs with a similar conformation but different size. *Aust Vet J*. 2000;78: 49-55.
51. Seckerdieck M, Holler P, Smets P, et al. Simpson's method of discs in Salukis and Whippets: echocardiographic reference intervals for end-diastolic and end-systolic left ventricular volumes. *J Vet Cardiol*. 2015; 17:271-281.
52. Jacobson JH, Boon JA, Bright JM. An echocardiographic study of healthy Border Collies with normal reference ranges for the breed. *J Vet Cardiol*. 2013;15:123-130.
53. Cunningham SM, Rush JE, Freeman LM, et al. Echocardiographic ratio indices in overtly healthy Boxer dogs screened for heart disease. *J Vet Intern Med*. 2008;22:924-930.

How to cite this article: Feldhütter EK, Domenech O, Vezzosi T, et al. Echocardiographic reference intervals for right ventricular indices, including 3-dimensional volume and 2-dimensional strain measurements in healthy dogs. *J Vet Intern Med*. 2022;36(1):8-19. doi:10.1111/jvim.16331